Surface Science 604 (2010) L67–L70

Contents lists available at ScienceDirect

Surface Science

journal homepage: www.elsevier.com/ locate/susc

Surface Science Letters

Misfit-dislocation-mediated heteroepitaxial island diffusion

A.W. Signor, Henry H. Wu, Dallas R. Trinkle *

Department of Materials Science and Engineering, University of Illinois, Urbana-Champaign, United States

ARTICLE INFO

Article history:
Received 12 February 2010
Accepted 2 August 2010
Available online 14 August 2010

Keywords:
Surface diffusion
Scanning tunneling microscopy
Molecular dynamics
Copper
Silver

ABSTRACT

Scanning tunneling microscopy combined with molecular dynamics simulations reveals a dislocation-mediated island diffusion mechanism for Cu on Ag(111), a highly mismatched system. Cluster motion is tracked with atomic precision at multiple temperatures and diffusion barriers and prefactors are determined from direct measurements of hop rates. The barrier to nucleate a dislocation is sensitive to island size and shape, resulting in a non-monotonic size dependence of the diffusion barrier.

1. Introduction

Dislocations are key in the mechanical properties of solids by enabling crystalline materials to deform plastically when subjected to stress orders of magnitude lower than their theoretical critical shear stress [1]. They have also been shown to relieve stress in strained films, greatly affecting the growth mode [2–4], and have been predicted [5,6] but never experimentally implicated in adatom island diffusion. The majority of experimental studies of island diffusion have been limited to homoepitaxial systems where motion is usually a result of diffusion at steps, particularly for large islands (10^2–10^3 atoms) [7–12]. In these cases, the barrier is insensitive to size, but diffusivity scales with size depending on the rate-limiting process [13–15]. In contrast, there have been numerous theoretical predictions [16–22] and a few experimental demonstrations [23–27] of non-trivial size dependencies of the diffusion *barrier and/or prefactor* for smaller homoepitaxial clusters (2–20 atoms). This work shows that dislocations in highly mismatched heteroepitaxial islands reduce barriers for islands of special sizes and shapes in the same way that they reduce the yield stress of bulk materials: by enabling slip to occur in a piecewise fashion.

Using scanning tunneling microscopy (STM) and molecular dynamics (MD) simulations, we reveal a dislocation-mediated island diffusion mechanism for Cu on Ag(111). Simulations show that the lattice mismatch of ~12% favors dislocation nucleation in islands larger than tetramers, resulting in a non-trivial size dependence that is manifest in experiments where clusters containing up to 26 diffuse much faster than smaller clusters. The barriers for island sizes and shapes favoring this mechanism are lower than that of edge diffusion or Ostwald ripening, and cluster coalescence is the kinetically preferred coarsening pathway.

Measurements were carried out in an Omicron LT-STM that can image at 4.5–300 K. The sample stage was enclosed by a cryogenically-cooled metal shroud which kept the temperature regulated and the sample clean. The Ag(111) substrate was prepared in an adjoining chamber by evaporating Ag onto Si(111)-7×7 at ~20 K and annealing at ~500 K for 1–2 h, producing large, defect-free terraces [28]. To test surface quality, diffusion barriers for atoms and dimers on these substrates were measured and are in good agreement with the published values of 65 and 73 meV, respectively [29]. The sample, held at 5 K on the STM stage, was exposed to Cu atoms. The Cu areal density, θ, was determined by counting atoms from images collected at 5 K. The STM stage was warmed to allow atom and dimer diffusion and cluster growth. From high-resolution images of a large (600) ensemble of clusters, sizes were estimated by measuring their area at *X*% of the cluster height. The precisely known Cu adatom density, θ, was used to adjust the parameter X until $A_{\text{image}}\theta = A_{\text{island}}\rho_{\text{Cu(111)}}$, where A_{image} is the area of the image, A_{island} is the total area of the island ensemble, and $\rho_{\text{Cu(111)}}$ is the areal density of a bulk Cu(111) plane. It is estimated that the uncertainty in island size is ± 1 atom.

The region of interest was imaged every 4.26 min for ~80 h at each temperature, 80, 83, 85, and 87 K. This enabled diffusion barriers and prefactors to be measured directly for individual clusters. Fig. 1 shows a sequence of STM images collected at 80 K. What is interesting is that the 13-atom cluster underwent significant diffusion, while the 7- and 15-atom clusters were immobile, suggesting a "magic" size with a low diffusion barrier. There was no change in size or shape, ruling out edge diffusion or atom exchange between islands—the apparent change in shape in Fig. 1 is a result of an increase in scan speed after the first image. The dotted line guides the eye along the diffusion path of the

* Corresponding author.
E-mail address: dtrinkle@illinois.edu (D.R. Trinkle).

0039-6028/$ – see front matter © 2010 Elsevier B.V. All rights reserved.
doi:10.1016/j.susc.2010.08.003

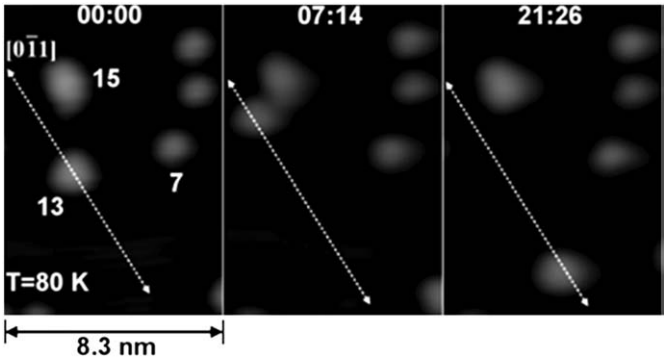

Fig. 1. STM images (−200 mV, 0.5 nA) at 80 K showing diffusion of a 13-atom Cu cluster on Ag(111). The relative times of the images are given in h:min. The arrow indicates a diffusion trajectory along $[0\bar{1}1]$. This cluster undergoes significant diffusion, while the neighboring 7- and 15-atom clusters are immobile.

13-atom cluster. That motion occurs along the close-packed $[0\bar{1}1]$ direction is significant because fcc metals slip on {111} planes in [110] directions, suggesting a relation between the diffusion mechanism and dislocation glide.

Using a particle tracking program [30], we determine trajectories with atomic precision, as shown in Fig. 2 for a 10-atom cluster at 85 K. The positions occupied by the cluster centroid are plotted vertically on the left, revealing a discrete set of adsorption sites separated by the Ag nearest-neighbor distance. This shows that the cluster hops collectively between equivalent sites. If diffusion occurred through individual atomic events, hop lengths for the centroid would be a fraction of this distance and inversely proportional to island size. Diffusion measurements for the cluster in Fig. 2 at 83, 85, and 87 K showed that it visited 9, 12, and 20 sites after 50, 120, and 230 hops, respectively. This demonstrates that the diffusion is close to an unrestricted 1-D random walk since the number of sites visited in a walk of n hops is expected to be $(8n/\pi)^{1/2}$, which yields 11, 17, and 24 sites for the cases above [31].

The plot of position vs. time in Fig. 2 shows that the mean time between hops is long compared to the frame rate, ensuring that all hops are counted and mean hop rates can be measured directly. The mean hop rate for this cluster at 83, 85, and 87 K is plotted against 1/kT in the inset, giving an activation energy of 260 ± 20 meV and a prefactor of $7 \times 10^{11 \pm 1.3}$ s^{-1}. The reported barrier, prefactor and related uncertainties were determined using a weighted least-squares fit, where the weighting factors and uncertainties were derived from the standard deviation of the measured time between hops and the number of hops observed [32]. Several 10-atom clusters were followed at multiple temperatures and all had barriers and prefactors within a standard error of 260 meV and 10^{12} s^{-1}.

The experiments show that low diffusion barriers are not limited to clusters larger than heptamers. Fig. 3 is a series of STM images showing the diffusion of a pentamer at 80 K. In this case, motion was too fast for direct hop rate measurement, but the number of distinct sites visited was determined to be 55. By assuming an unrestricted random walk with a prefactor of 10^{12} s^{-1}, the barrier was estimated to be ~210 meV. Similar measurements for 13-, 14- and 26-atom clusters at 83 K give barriers of 225, 240 and 250 meV, respectively, showing that this mechanism is viable beyond the decamer. In comparison, these diffusion barriers are much lower than the barriers for homoepitaxial island migration through edge diffusion on either Cu(111) or Ag(111), ~500 meV [12] and in the size range studied, coarsening through cluster–cluster coalescence is kinetically favored over Ostwald ripening [33–38]. The non-monotonic size dependence of the diffusion barrier is clearly more complex than the simple single magic size effect predicted by Hamilton [6] for a mismatched system.

MD simulations were conducted to investigate the atomic processes at work. An embedded-atom method potential parameterized for Cu/Ag(111) [39] determines the diffusion barriers and mechanisms for selected islands. This potential overestimates the monomer and dimer diffusion barriers, giving 93 and 88 meV, which are 10–15 meV above the experimental measurements [29]. The potential is optimized to produce accurate island geometries, energies, and kinetics. High-temperature annealing allows the equilibrium island shapes to be determined. Molecular dynamics simulations and dimer method [40] search the phase-space for possible diffusion transitions, and the nudged-elastic band method [41] determines the energy barriers and the atomic-scale mechanisms.

Fig. 4 summarizes the MD results for 3-, 7-, 5-, and 10-atom clusters, which show that islands of certain sizes and shapes allow metastable dislocations, leading to reduced diffusion barriers. The trimer in Fig. 4(a) moves through simultaneous glide with a barrier of 287 meV, roughly three times the simulated monomer diffusion barrier. The heptamer (Fig. 4(b)) also moves in a collective fashion, though the atoms do not cross bridge sites simultaneously. In the transition state, the top right portion of the island moves towards hcp stacking prior to the lower left, reducing the barrier to 490 meV, about five times the monomer barrier.

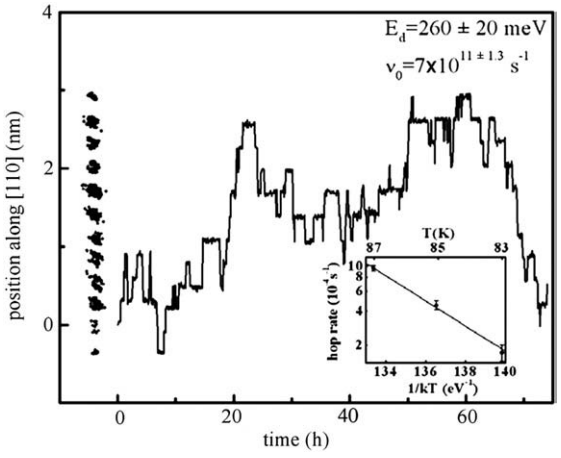

Fig. 2. Diffusion trajectory for a 10-atom cluster doing a 1-D walk along [110]at 85 K. Each point on the left represents the cluster's centroid from a data set containing ~1100 frames. The plot as a function of time makes it possible to determine the mean hop rate. In the inset, the temperature dependence of the hop rate yields an activation energy of 260 ± 20 meV, and an attempt frequency of $7 \times 10^{11 \pm 1.3}$ s^{-1}.

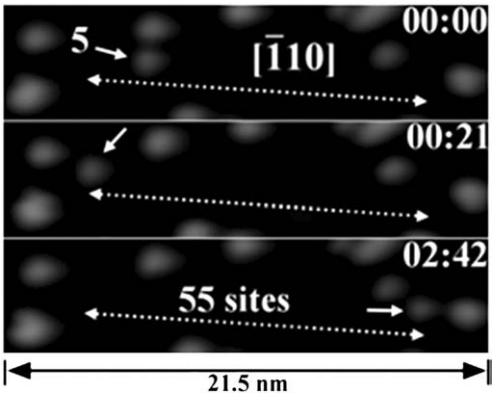

Fig. 3. STM images (−200 mV, 0.5 nA) showing diffusion of a 5-atom cluster at 80 K. The relative times of the images are given in h:min. While pentamer diffusion at 80 K was too fast for direct hop rate determination, the barrier was estimated to be ~210 meV, assuming an unrestricted random walk.

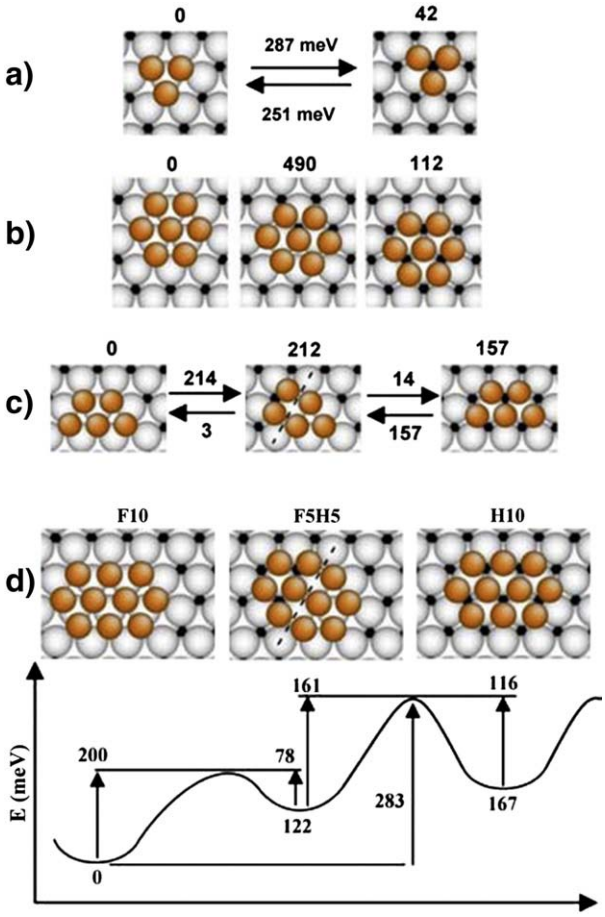

Fig. 4. Molecular dynamics simulations of 3-, 7-, 5-, and 10-atom Cu clusters on Ag(111). The trimer (a) migrates via simultaneous glide, with all atoms moving across bridge sites at the same time. The heptamer (b) moves in a dislocation-like mechanism, where the transition state contains atoms in both fcc and hcp sites. The pentamer (c) and decamer (d) diffuse via a different misfit dislocation mechanism, where the states containing the dislocation are metastable and the dislocation lines are oriented along [110]. All energy values are given in meV.

Fig. 4(c) and (d) shows that a different, low-barrier mechanism involving a metastable dislocation (dotted lines) is accessible to the pentamer and decamer. The diffusion barrier for the decamer, 283 meV, is little more than half that of the heptamer and even slightly lower than the trimer barrier. The pentamer and decamer diffusion barriers, 214 and 283 meV, respectively, are in excellent agreement with the experimental values of ~210 and 260 ± 20 meV. The overestimation of the barriers in the simulations is expected, based on the monomer and dimer simulation barriers. The diffusion process for the decamer in Fig. 4(d) proceeds as follows. Starting from F10, all Cu atoms in fcc sites, a metastable state with 5 atoms in hcp sites, F5H5, is accessed. The dashed line indicates a dislocation with Burgers vector $\vec{b} = 1/6[\bar{2}11]$ separating the fcc and hcp regions. If the remaining fcc atoms follow to H10, the center of mass is displaced by one Burgers vector. Symmetry allows F10 to accommodate dislocations with $\vec{b} = 1/6[\bar{2}11]$ or $\vec{b} = 1/6[1\bar{2}1]$ while H10 can accommodate $\vec{b} = 1/6[\bar{1}2\bar{1}]$ or $\vec{b} = 1/6[2\bar{1}\bar{1}]$. Thus, successive dislocation events allow for forward, backward, or zero net displacement along $[\bar{1}10]$ with equal probability and a barrier of 283 meV for a complete fcc–fcc step. This type of motion is similar to what has been called "reptation" [42,43]. The short lifetimes of H10 ($\sim 10^{-4}$ s) and H5F5 ($\sim 10^{-8}$ s) compared to F10 (on the order of seconds) would prevent them from being observed with STM and any image of the cluster would show it in the F10 configuration. The pentamer (Fig. 4(c)) moves in an analogous manner. Despite the 3-fold symmetry of fcc {111}, the experimental trajectories presented in this paper show one-dimensional motion; however, many islands throughout the size range diffused in two dimensions with varying degrees of anisotropy from completely isotropic to highly anisotropic. This is possibly due to differing local environments resulting from cluster–cluster interactions.

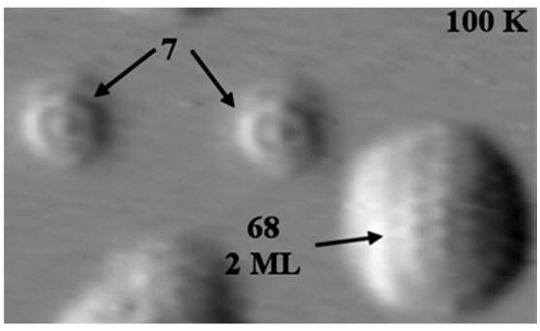

Fig. 5. Atomic resolution image at 100 K after a ~90 s anneal at ~200 K. Heptamers survived the anneal and were immobile at 100 K. The other clusters on the surface contained 20 or more atoms, having formed from cluster–cluster coalescence. Many bilayer islands were present, like the 68-atom island shown.

More extensive simulations show that the low-barrier mechanism, as shown for the decamer and pentamer in Fig. 4, is inaccessible to closed-shell structures like the trimer and heptamer. To preserve Cu–Cu bonds, the dislocations in this process must nucleate between close-packed rows of the same length and with Burgers vectors that bring the atoms closer together [44]. This is why the only dislocations allowed in the F10 or H10 configurations are $1/6[\bar{2}11]$,$1/6[1\bar{2}1]$ or their directional opposites. This rule means that besides island size, shape is important. There is an indication in the experimental measurements that shape can be as important as size because some initially-immobile clusters are spontaneously mobilized subsequent to a shape change while maintaining their size.

Our diffusion model is further supported by the image in Fig. 5 collected at 100 K after a 90-second anneal to ~200 K which allowed significant coarsening. The features within the clusters have the orientation and lattice spacing expected for Cu on Ag(111) and we interpret this to be an atomic resolution of the clusters, allowing precise determination of size. The image shows monolayer-tall heptamers as well as a two-layer 68-atom island in epitaxial orientation with the substrate. The slight halos around the clusters are likely a result of the finite size and shape of the tip rather than being real features of the surface. Many heptamers were present after the anneal and were immobile at 100 K, while all other islands (many multi-layer) contained 20 or more atoms. We interpret the presence of the heptamers after the anneal as an indication of their low mobility relative to other clusters with sizes up to ~20 atoms, consistent with simulations that predict the heptamer to have the highest diffusion barrier among clusters containing up to 14 atoms. Though it is possible that the heptamers were trapped at undetectable defects, such trapping would be expected to immobilize clusters of all sizes.

We have shown that a dislocation mechanism provides a pathway to coarsening through cluster diffusion for clusters as large as 26 atoms with barriers significantly lower than those of edge diffusion or Ostwald ripening. This mechanism leads to significantly reduced diffusion barriers for islands with sizes and shapes that favor metastable dislocations with the result that large islands can move more easily than smaller ones. Thus, in much the same way that dislocations reduce the yield stress of bulk metals from their theoretical values, they also reduce island diffusion barriers. It is clear that this mechanism is promoted by lattice mismatch, which reduces the energy cost of bringing the Cu atoms closer together, and it is likely a general phenomenon applicable to similarly mismatched systems.

Acknowledgements

We thank J. H. Weaver, R. E. Butera, P. Swaminathan, C. M. Aldao, and G. Ehrlich for their valuable discussions. This work is supported by NSF/DMR grant 0703995.

References

[1] D. Hull, D.J. Bacon, 4th ed., Butterworth-Heinemann, 2001.
[2] M. Krishnamurthy, J.S. Drucker, J.A. Venables, J. Appl. Phys. 69 (1991) 6461.
[3] D.J. Eaglesham, M. Cerullo, Phys. Rev. Lett. 64 (1990) 1943.
[4] J. Drucker, Phys. Rev. B 48 (1993) 18203.
[5] J.C. Hamilton, M.S. Daw, S.M. Foiles, Phys. Rev. Lett. 74 (1995) 2760.
[6] J.C. Hamilton, Phys. Rev. Lett. 77 (1996) 885.
[7] K. Morgenstern, Phys. Status Solidi B 242 (2005) 773.
[8] M. Giesen, Prog. Surf. Sci. 68 (2001) 1.
[9] K. Morgenstern, E. Laegsgaard, F. Besenbacher, Phys. Rev. Lett. 86 (2001) 5739.
[10] K. Morgenstern, G. Rosenfeld, B. Poelsema, G. Comsa, Phys. Rev. Lett. 74 (1995) 2058.
[11] J.–.M. Wen, S.L. Chang, J.W. Burnett, J.W. Evans, P.A. Thiel, Phys. Rev. Lett. 73 (1994) 2591.
[12] D.C. Schlößer, et al., Surf. Sci. 465 (2000) 19.
[13] K. Morgenstern, E. Lægsgaard, F. Besenbacher, Phys. Rev. B 66 (2002) 115408.
[14] S.V. Khare, N.C. Bartelt, T.L. Einstein, Phys. Rev. Lett. 75 (1995) 2148.
[15] S.V. Khare, T.L. Einstein, Phys. Rev. B 54 (1996) 11752.
[16] A. Karim, A.N. Al-Rawi, A. Kara, T.S. Rahman, Phys. Rev. B 73 (2006) 165411.
[17] J. Heinonen, I. Koponen, J. Merikoski, T. Ala-Nissila, Phys. Rev. Lett. 82 (1999) 2733.
[18] V. Papathanakos, G.A. Evangelakis, Surf. Sci. 499 (2002) 229.
[19] O.S. Trushin, P. Salo, T. Ala-Nissila, Phys. Rev. B. 62 (2000) 1611.
[20] O.S. Trushin, P. Salo, T. Ala-Nissila, Surf. Sci. 482–485 (2001) 365.
[21] C.M. Chang, C.M. Wei, S.P. Chen, Phys. Rev. Lett. 85 (2000) 1044.
[22] U. Kurpick, B. Fricke, G. Ehrlich, Surf. Sci. 470 (2000) L45.
[23] G.L. Kellogg, Phys. Rev. Lett. 73 (1994) 1833.
[24] S.C. Wang, G. Ehrlich, Surf. Sci. 239 (1990) 301.
[25] G.L. Kellogg, Appl. Surf. Sci. 67 (1992) 134.
[26] H.-W. Fink, G. Ehrlich, Surf. Sci. 150 (1985) 419.
[27] S.C. Wang, U. Kurpick, G. Ehrlich, Phys. Rev. Lett. 81 (1998) 4923.
[28] L. Huang, S.J. Chey, J.H. Weaver, Surf. Sci. 416 (1998) L1101.
[29] K. Morgenstern, K.-F. Braun, K.-H. Rieder, Phys. Rev. Lett. 93 (2004) 056102.
[30] J.C. Crocker, D.G. Grier, J. Colloid Interface Sci. 179 (1996) 298.
[31] J. Rudnick, G. Gaspari, Elements of the Random Walk, Cambridge University Press, 2004, pp. 63–67.
[32] R.J. Cvetanovic, D.L. Singleton, J. Phys. Chem. 83 (1979) 50.
[33] J.M. Wen, J.W. Evans, M.C. Bartelt, J.W. Burnett, P.A. Thiel, Phys. Rev. Lett. 76 (1996) 652.
[34] K. Morgenstern, G. Rosenfeld, G. Comsa, Phys. Rev. Lett. 76 (1996) 2113.
[35] K. Morgenstern, et al., Phys. Rev. Lett. 80 (1998) 556.
[36] G.S. Icking-Konert, M. Giesen, H. Ibach, Surf. Sci. 398 (1998) 37.
[37] J.B. Hannon, et al., Phys. Rev. Lett. 79 (1997) 2506.
[38] G. Rosenfeld, et al., Surf. Sci. 402 (1998) 401.
[39] H.H. Wu, D.R. Trinkle, Comput. Mater. Sci. 47 (2009) 577.
[40] G. Henkelman, H. Jónsson, J. Chem. Phys. 111 (1999) 7010.
[41] G. Mills, H. Jónsson, Phys. Rev. Lett. 72 (1994) 1124.
[42] V. Chirita, E. Munger, J. Greene, J.-E. Sundgren, Surf. Sci. Lett. 436 (1999) L641.
[43] V. Chirita, E. Munger, J. Greene, J.-E. Sundgren, Thin Solid Films 370 (2000) 179.
[44] H.H. Wu, A.W. Signor, D.R. Trinkle, J. Appl. Phys. 108 (2010) 023521.